Floquet Gauge Pumps as Sensors for Spectral Degeneracies Protected by Symmetry or Topology

Abhishek Kumar,[1] Gerardo Ortiz,[1,2] Philip Richerme,[1,2] and Babak Seradjeh[1,2,3]
[1]Department of Physics, Indiana University, Bloomington, Indiana 47405, USA
[2]Quantum Science and Engineering Center, Indiana University, Bloomington, Indiana 47405, USA
[3]IU Center for Spacetime Symmetries, Indiana University, Bloomington, Indiana 47405, USA

(Received 19 December 2020; accepted 16 April 2021; published 20 May 2021)

We introduce the concept of a Floquet gauge pump whereby a dynamically engineered Floquet Hamiltonian is employed to reveal the inherent degeneracy of the ground state in interacting systems. We demonstrate this concept in a one-dimensional XY model with periodically driven couplings and transverse field. In the high-frequency limit, we obtain the Floquet Hamiltonian consisting of the static XY and dynamically generated Dzyaloshinsky-Moriya interaction (DMI) terms. The dynamically generated magnetization current depends on the phases of complex coupling terms, with the XY interaction as the real and DMI as the imaginary part. As these phases are cycled, the current reveals the ground-state degeneracies that distinguish the ordered and disordered phases. We discuss experimental requirements needed to realize the Floquet gauge pump in a synthetic quantum spin system of interacting trapped ions.

DOI: 10.1103/PhysRevLett.126.206602

Introduction.—The nontrivial topology of gapped phases of matter is often manifested in states or modes localized at the boundary or defects of the system protected by symmetries and the bulk topological gap. This bulk-boundary correspondence has been rigorously proven in certain cases, especially in noninteracting systems [1–7]. Thus, the presence and properties of boundary modes is used as a telltale experimental signature of bulk topology [8]. However, boundary modes can arise in many other topologically trivial cases as well [9]. Moreover, the structure of boundary modes is far from clear in generic interacting many-body systems [10–13]. Therefore, more robust probes of bulk topology are highly sought after [14–19].

An example is provided by the fractional Josephson current J_s between topological superconductors supporting Majorana bound states as the phase difference $\Delta\phi$ between the superconductors is cycled by changing the magnetic flux enclosed by the system [20–23]. Unlike the Cooper-pair-mediated conventional Josephson current between trivial superconductors $J_s \propto \sin\Delta\phi$, the fractional Josephson current is dominated by quasiparticle tunneling through the Majorana bound states, $J_s \propto \sin(\Delta\phi/2)$. In the presence of interactions, the fractional Josephson current probes the topological degeneracy of the interacting ground state in a given fermion parity sector [11].

In this Letter, we consider a general spatially resolved probe provided by the variations in the current flowing through the bridge between two gapped phases as a relevant gauge field is varied in a cycle. Ground-state degeneracies through this cycle produce an anomalous periodicity of the corresponding current on the cycle parameters [24,25]. As energy is pumped through the junction, we call such probes "gauge pumps." In a topological phase, degeneracies are produced by topological boundary modes localized at the bridge. However, it is important to note that the role of bulk topology here is to guarantee the existence of degeneracies in the many-body spectrum. While the notion of topology depends on the choice of the local basis, or language, the existence of a many-body degeneracy is independent of this representation. Thus, depending on the local basis, gauge pumps can detect ground-state degeneracies of bulk topological or spontaneous symmetry broken phases.

We extend the notion of gauge pumps to periodically driven systems. We introduce the "Floquet gauge pump" realized by a periodic drive protocol that both imprints and controls the bridge geometry. As a concrete demonstration, we study the driven XY model in transverse field and show how Dzyaloshinsky-Moriya interaction (DMI) terms can be dynamically generated and tuned by the periodic drive. Upon Jordan-Wigner transformation [26], the DMI and exchange couplings map to complex fermion hopping and pairing amplitudes that realize trivial and topological superconducting phases of fermions corresponding, respectively, to disordered and ordered phases of the original spins. The spatial profile of the drive can be used both to create the bridge geometry of a gauge pump and to cycle its gauge parameters [27]. In the original spin model, the gauge current corresponds to the rate of change of magnetization. Thus, many-body degeneracies are revealed by an anomalous dependence of magnetization current on drive parameters. The gauge pump and its Floquet realization proposed in this Letter offer a powerful and widely

useful probe of symmetry-protected degeneracies of topological and ordered phases of quantum matter.

Floquet gauge pump.—A gauge pump is realized by a cyclic Hamiltonian $H(\phi)$ in the gauge parameters ϕ [31]. A constant ϕ can be gauged away as $U_g^\dagger(\phi)H(\phi)U_g(\phi) = H(0)$ with a unitary gauge transformation $U_g(\phi)$. The gauge pump is constructed by "bridging" two such Hamiltonians, H_L and H_R, to form $H_{\rm gp} = H_L(\phi_L)\otimes \mathbb{1}_R + H_{LR} + \mathbb{1}_L \otimes H_R(\phi_R)$, where $\mathbb{1}_{L(R)}$ is the identity operator on the left (right) side of the bridge given by H_{LR}. After a gauge transformation $U_g = U_{gL}(\phi_L)\otimes U_{gR}(\phi_R)$, we have the gauge-equivalent Hamiltonian $U_g^\dagger H_{\rm gp} U_g = H_L(0)\otimes \mathbb{1}_R + H_b(\phi_h,\phi_p) + \mathbb{1}_L \otimes H_R(0)$, where $\phi_h \equiv \phi_L - \phi_R$, $\phi_p \equiv \phi_L + \phi_R$, and $H_b = U_g^\dagger H_{LR} U_g$. Then, the gauge currents on each side are [33]

$$j_L \coloneqq \left\langle \frac{\partial H_{\rm gp}}{\partial \phi_L}\right\rangle = \left\langle \frac{\partial H_b}{\partial \phi_p}\right\rangle_g + \left\langle \frac{\partial H_b}{\partial \phi_h}\right\rangle_g, \tag{1}$$

$$j_R \coloneqq \left\langle \frac{\partial H_{\rm gp}}{\partial \phi_R}\right\rangle = \left\langle \frac{\partial H_b}{\partial \phi_p}\right\rangle_g - \left\langle \frac{\partial H_b}{\partial \phi_h}\right\rangle_g, \tag{2}$$

where the expectation values $\langle\cdots\rangle_g = \langle U_g\cdots U_g^\dagger\rangle$. Note that the current flow is set with respect to the bridge, so the positive values have opposite directions on each side. If the bridge Hamiltonian H_b is a function of ϕ_h only, the two currents $j_L = -j_R$ and no gauge charge is accumulated in the bridge itself. However, if the bridge Hamiltonian also depends on ϕ_p, then $j_b \coloneqq j_L + j_R = 2\langle \partial H_b/\partial\phi_p\rangle_g$ must be carried by the bridge itself. If the bridge is "grounded," e.g., in a transport geometry of a mesoscopic device, this can flow through the bridge. Otherwise, the gauge charge will accumulate in the bridge.

The Floquet gauge pump provides two complementary functions. First, as we show, periodic drive protocols with spatial variations may be used both to engineer the gauge parameters and to imprint the gauge pump geometry [28–30]. Second, drive parameters can be tuned to engineer Floquet topological phases of the system [34–46]. The signatures of both equilibrium and Floquet topological phases can then be probed by the dependence of the gauge current pumped through the system on tunable gauge parameters. To illustrate this, note that the stroboscopic dynamics of the driven Hamiltonian $H_{\rm gp}(t) = H_L(t)\otimes \mathbb{1}_R + H_{LR}(t) + \mathbb{1}_L \otimes H_R(t) = H_{\rm gp}(t + 2\pi/\Omega)$ with drive frequency Ω is governed by the Floquet Hamiltonian [47–49] $H_{\rm gp}^F = i(\Omega/2\pi)\ln {\rm Texp}[-i\oint H_{\rm gp}(t)dt] \equiv H_L^F \otimes \mathbb{1}_R + H_{LR}^F + \mathbb{1}_L \otimes H_R^F$, where the time-ordered exponential Texp is over a full cycle of the drive and we have set Planck's constant $\hbar = 1$. At high frequency up to $\mathcal{O}(\Omega^{-2})$, we may expand [50,51] $H_a^F = H_a^{(0)} + \sum_{n\in\mathbb{N}}[H_a^{(-n)}, H_a^{(n)}]/(n\Omega)$ for $a = L$, R and

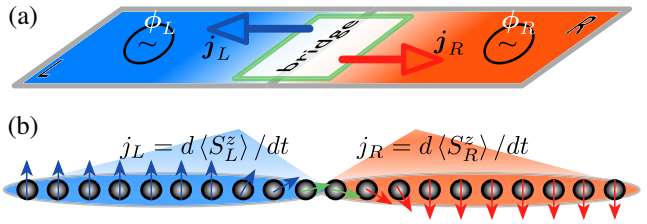

FIG. 1. Sketch of the Floquet gauge pump and its ion-trap realization. (a) By periodically driving the left (L) and right (R) sides of the system with different gauge parameters ϕ_L and ϕ_R, the pump geometry and currents j_L and j_R can be engineered and controlled. (b) Trapped ions can realize a Floquet gauge pump with effective spin degrees of freedom, in which magnetization currents $d\langle S_{L,R}^z\rangle/dt$ can be pumped by controlling the drive protocols on each side.

$$H_{LR}^F = H_{LR}^{(0)} + \sum_{n\in\mathbb{N}}\left\{\frac{[H_{LR}^{(-n)}, H_{LR}^{(n)}]}{n\Omega} + \sum_a\left(\frac{[H_{LR}^{(-n)}, H_a^{(n)}]}{n\Omega} + {\rm H.c.}\right)\right\}, \tag{3}$$

where $O^{(n)} = (\Omega/2\pi)\oint O(t)e^{in\Omega t}dt$ are the Fourier components of operator O and H.c. is the Hermitian conjugate. We denote the gauge parameters in this Floquet Hamiltonian as $\phi_L(\lambda)$ and $\phi_R(\lambda)$ with λ denoting the drive parameters, such as frequency, harmonic amplitudes, and phases. The twofold function of the Floquet gauge pump is then to provide independent realizations and tuning of ϕ_L and ϕ_R. Figure 1 sketches our setup.

The gauge currents $j_a(t) = \langle \partial H_{\rm gp}(t)/\partial\phi_a\rangle$ are now time dependent. We show in the Supplemental Material [33] that, if the expectation value is calculated in Floquet modes $|\Psi(t)\rangle = e^{-i\epsilon t}|\Phi(t)\rangle$, where ϵ is the quasienergy and $|\Phi(t + 2\pi/\Omega)\rangle = |\Phi(t)\rangle$ is the periodic eigenstate satisfying $[H_{\rm gp}(t) - i\partial/\partial t]|\Phi(t)\rangle = \epsilon|\Phi(t)\rangle$, then the average gauge current is

$$j_a^{(0)} = \frac{\partial\epsilon}{\partial\phi_a}. \tag{4}$$

The choice of physical state of the driven system requires care. Generic driven systems would, at infinitely long times, settle into a uniform mixed state by absorbing energy from the drive without bound [52,53], with the exception of integrable or many-body localized systems [54–58]. However, at intermediate times that can be extremely long for sufficiently large systems, the Floquet state describes the dynamics of the system rather well [59–63]. At high enough frequency, in particular, an initial equilibrium state of the average Hamiltonian $H_{\rm gp}^{(0)}$ is nearly the same as the Floquet state. In the following, we will assume that this is indeed the case and calculate gauge currents from the Floquet spectrum.

Spin model.—To illustrate the concepts, here we consider a driven XY model in a transverse field $H_{XY}(t)=\sum_j[J_j^x(t)S_j^xS_{j+1}^x+J_j^y(t)S_j^yS_{j+1}^y+h_j^z(t)S_j^z]$, where $\{S_j^x,S_j^y,S_j^z\}$ are spin-$\frac{1}{2}$ operators, $\{J_j^x,J_j^y\}$ are nearest-neighbor couplings, and h_j^z is the transverse field at lattice site j. We take the periodic drive to be independent and uniform on each side with $J_{j\in a}^{x,y}(t)=\bar{J}_a^{x,y}+\delta J_a^{x,y}\cos(\Omega t+\theta^J)$, and $h_a^z(t)=\bar{h}_a^z+\delta h_a^z\cos(\Omega t+\theta_a^h)$. With this choice, the high-frequency Floquet Hamiltonian takes the form [33] $H_{XY}^F=H_L^F+H_{LR}^F+H_R^F+\mathcal{O}(\Omega^{-2})$,

$$H_a^F=\bar{H}_a+\sum_{j\in a}\zeta_a(S_j^xS_{j+1}^y+S_j^yS_{j+1}^x), \tag{5}$$

$$H_{LR}^F=\bar{H}_{LR}+\zeta_{LR}(S_\ell^xS_r^y+S_\ell^yS_r^x)+\xi_{LR}(S_\ell^xS_r^y-S_\ell^yS_r^x). \tag{6}$$

Here $\bar{H}_a$ is the average Hamiltonian on side a and $\zeta_a=-\delta J_a^-\delta h_a^z\sin(\theta_a^h-\theta^J)/\Omega$ with $\delta J_a^\pm=(\delta J_a^x\pm\delta J_a^y)/2$. At the junction connecting the sites $\ell\in L$ and $r\in R$, $\bar{H}_{LR}$ is the contribution from the averaged Hamiltonian, $\zeta_{LR}=-\delta J_L^-[\sin(\theta_R^h-\theta^J)\delta h_R^z+\sin(\theta_L^h-\theta^J)\delta h_L^z]/(2\Omega)$, and $\xi_{LR}=\delta J_L^+[\sin(\theta_R^h-\theta^J)\delta h_R^z-\sin(\theta_L^h-\theta^J)\delta h_L^z]/(2\Omega)$ is the DMI term dynamically generated by the drive. The z component of the magnetization current on side a is defined as $j_a=d\langle S_a^z\rangle/dt$, where $S_a^z=\sum_{j\in a}S_j^z$.

It is mathematically convenient to analyze the spin gauge pump in the dual fermionic language. To this end, we employ the Jordan-Wigner transformation [26] $S_j^x+iS_j^y=P_jc_j^\dagger$, $S_j^z=n_j-\frac{1}{2}$, with number operator $n_j=c_j^\dagger c_j$ ($c_j,c_j^\dagger$ are fermionic operators) at site j, and $P_j=\prod_{l<j}e^{i\pi n_l}$ as the fermion parity to the left of site j. This is followed by the gauge transformation $e^{i\phi_a}c_j^\dagger\to c_j^\dagger$ for $j\in a$, to find, up to a constant, the equivalent fermion Hamiltonian $\tilde{H}_L^F+H_b+\tilde{H}_R^F$,

$$\tilde{H}_a^F=\sum_{j\in a}[w_ac_j^\dagger c_{j+1}+\Delta_ac_j^\dagger c_{j+1}^\dagger+\mu_an_j]+\text{H.c.}, \tag{7}$$

$$H_b=w_be^{i\phi_h}c_\ell^\dagger c_r+\Delta_be^{i\phi_p}c_\ell^\dagger c_r^\dagger+\text{H.c.}, \tag{8}$$

where chemical potential $\mu_a=\frac{1}{2}h_a^z$, hopping amplitudes $w_a=\frac{1}{2}J_a^+$ and $w_b=\frac{1}{2}|(J_L^++i\xi_{LR})|$, and pairing amplitudes $\Delta_a=\frac{1}{2}|(J_a^-+i\zeta_a)|$ and $\Delta_b=\frac{1}{2}|(J_L^-+i\zeta_{LR})|$, $J_a^\pm=(\bar{J}_a^x\pm\bar{J}_a^y)/2$ are all real, and

$$\phi_h=\phi_{hb}+(\phi_L-\phi_R), \tag{9}$$

$$\phi_p=\phi_{pb}+(\phi_L+\phi_R), \tag{10}$$

with $\phi_a=\frac{1}{2}\arg(J_a^-+i\zeta_a)$ half of the pairing phase on each side, $\phi_{hb}=\arg(J_L^++i\xi_{LR})$ and $\phi_{pb}=\arg(J_L^-+i\zeta_{LR})$.

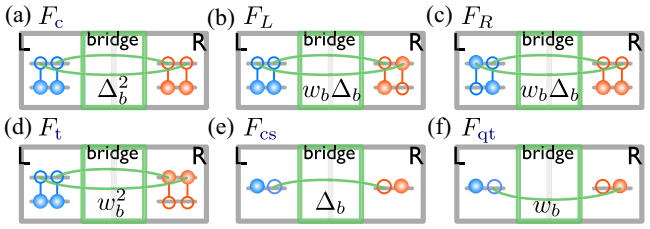

FIG. 2. Gauge current processes. In the trivial phase (a)–(d), second-order virtual processes due to pairing $\Delta_bc_\ell^\dagger c_r^\dagger$ (hopping $w_bc_\ell^\dagger c_r$ or $w_bc_\ell c_r^\dagger$) tunneling are shown by ● (○ or ●) in L and ● (○ or ●) in R: (a) Cooper pair cotunneling; (b),(c) Cooper pair condensation; (d) Cooper pair tunneling. In the topological phase (e),(f) the direct tunneling via Majorana bound states contributes by (e) Cooper pair splitting and (f) quasiparticle tunneling.

This fermionic Hamiltonian is composed of a Kitaev chain [20] on each side and a bridge Hamiltonian with both hopping and pairing terms at the junction, thus realizing an unconventional Josephson junction that can be controlled by the original drive parameters. In terms of fermions, the currents $j_a=d\langle N_a\rangle/dt$, where $N_a=\sum_{j\in a}n_j$ is the fermion number operator on side a.

The Kitaev chain has two phases. For $|\mu_a|<2w_a$, there are unpaired Majorana bound states at the junction and the spectrum is doubly degenerate. In terms of spins, this corresponds to the ordered phase of the XY model. By contrast, when $|\mu_a|>2w_a$, the spectrum is nondegenerate and corresponds to a disordered spin chain. The presence or absence of Majorana fermions at the junction affects the current across the junction.

Floquet gauge current.—The average Floquet gauge current is given by Eq. (4), which requires the calculation of the quasienergies of H_{XY}^F. We will do so perturbatively in the bridge Hamiltonian, where the unperturbed system (without the bridge) has a Floquet spectrum $|\Phi_\alpha\rangle$ with quasienergies ϵ_α. The quasienergy of a state $|\Phi_{\alpha=0}\rangle$ in second-order perturbation theory is $\epsilon=\epsilon_0+\epsilon_b$, where $\epsilon_b(\phi_h,\phi_p)=\langle\Phi_0|H_b|\Phi_0\rangle+\sum_{\alpha\neq0}|\langle\Phi_0|H_b|\Phi_\alpha\rangle|^2/(\epsilon_0-\epsilon_\alpha)$. We present the details of this calculation in the Supplemental Material [33] and quote the main results here.

In the trivial (disordered) phase, the first-order contribution vanishes since H_b projects out of the unperturbed ground state. Then the current takes the form

$$j_L^{(0)}=F_c\sin(2\phi_p)+F_L\sin(\phi_p+\phi_h)+F_t\sin(2\phi_h), \tag{11}$$

$$j_R^{(0)}=F_c\sin(2\phi_p)+F_R\sin(\phi_p-\phi_h)-F_t\sin(2\phi_h), \tag{12}$$

where $F_c\propto\Delta_b^2$, $F_{L,R}\propto w_b\Delta_b$, and $F_t\propto w_b^2$ are second order in bridge tunneling amplitudes. The parity of the nondegenerate state is fixed over the entire range of gauge parameters.

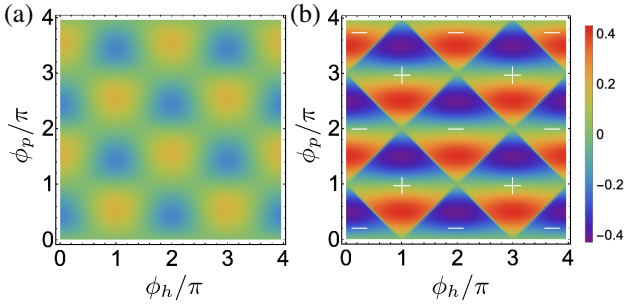

FIG. 3. The gauge current $j_b = j_L + j_R$ through the bridge, scaled as j_b/w_b^2 in the trivial phase (a) and j_b/w_b in the topological phase (b). The parity of the ground state is fixed in the trivial phase (a), but switches sign in the topological phase (b). The parameters are $w_L = w_R = 1$ (units of energy), $\Delta_L = \Delta_R = 0.5, \Delta_b = w_b = 0.2$; $\mu_L = \mu_R = 2.15$ in (a) and $\mu_L = \mu_R = 1.8$ in (b).

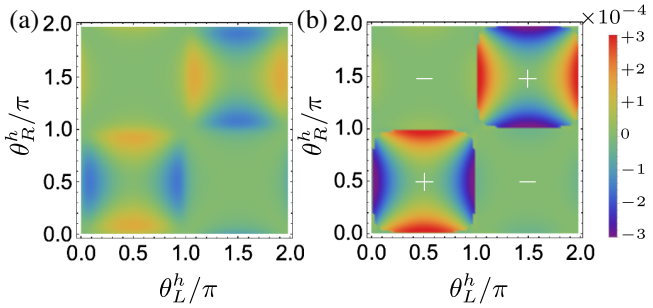

FIG. 4. The magnetization current $d\langle S_b^z\rangle/dt$ in units of Ω, at the bridge, $S_b^z = S_L^z + S_R^z$, for (a) disordered and (b) ordered phases of the driven XY model. The correlator $\langle\prod_j(-2S_j^z)\rangle$ is fixed in (a) and switches sign in (b). In units of Ω, the parameters are $\bar{J}_L^x = \bar{J}_R^x = 1.1\times10^{-4}, \bar{J}_L^y = \bar{J}_R^y = 10^{-5}, \delta J_L^x = \delta J_R^x = 3.2\times10^{-2}$, $\delta J_L^y = \delta J_R^y = 2\times10^{-3}, \theta^J = 0, \delta h_L^z = -\delta h_R^z = 0.03$. In (a) $\bar{h}_L^z = \bar{h}_R^z = 3\times10^{-4}$; in (b) $\bar{h}_L^z = \bar{h}_R^z = 10^{-4}$.

We illustrate the processes contributing to gauge currents in this case in Figs. 2(a)–2(d). For $\Delta_b = 0, w_b \neq 0$ we have the conventional Josephson junction and the current $j_L = -j_R = F_t \sin(2\phi_h)$ mediated by Cooper pair tunneling across the bridge. When $\Delta_b \neq 0, w_b = 0$, the currents $j_L = j_R = F_c \sin(2\phi_p)$ are mediated by Cooper pair cotunneling to or from the bridge. In the general case, $\Delta_b, w_b \neq 0$, the current j_a contain cross terms $\sim\sin(\phi_p \pm \phi_h)$, contributed by Cooper pair condensation at the bridge. Remarkably, in this case, the period of the Josephson current in ϕ_h and ϕ_p is doubled, similar to the junction with Majorana fermions and conserved fermion parity (see below) [64].

In the topological (ordered) phase, the first-order contribution dominates since H_b can now connect the unperturbed degenerate states. Then [33]

$$j_L^{(0)} = P_0(F_{cs}\sin\phi_p + F_{qt}\sin\phi_h), \tag{13}$$

$$j_R^{(0)} = P_0(F_{cs}\sin\phi_p - F_{qt}\sin\phi_h), \tag{14}$$

where $F_{cs} \propto \Delta_b$ and $F_{qt} \propto w_b$ are linear in the bridge tunneling amplitudes, and $P_0 = \langle\Phi_0|P|\Phi_0\rangle$, where $P = \prod_j e^{i\pi n_j}$, is the parity of the state $|\Phi_0\rangle$ in the doubly degenerate manifold. Note that $\epsilon_b/P_0 = -(F_{cs}\cos\phi_p + F_{qt}\cos\phi_h)$ switches sign in the cycle [33]. The term $\sim\sin\phi_h$ is the fractional Josephson current mediated by Majorana quasiparticle tunneling across the bridge [22]. The term $\sim\sin\phi_p$ is an unconventional Josephson current mediated by Cooper pair splitting at the bridge [65]; see Figs. 2(e) and 2(f).

The two phases of the spin system can thus be distinguished by the Floquet gauge current in two ways: (i) the linear (ordered) vs quadratic (disordered) dependence of the gauge current on the bridge tunneling amplitudes, and (ii) the dependence of the current on ϕ_h and ϕ_p. The latter is often formulated as doubling of the periodicity of the current in the topological vs trivial phase of fermions. This, in turn, relies on the conservation of the parity P_0 of the fermionic ground state. If, instead, the system is prepared with the same sign of ϵ_b, the parity of the ground state exhibits switches accompanied by discontinuities in the gauge current at topologically protected degeneracies in the topological phase, which are absent in the trivial phase.

In terms of spins, the parity operator $P = \exp[i\pi\sum_j(S_j^z + 1/2)] = \prod_j(-2S_j^z)$. Therefore, the total fermion parity is the maximal multipoint spin-z correlator. If the spin state is independently prepared for each value of ϕ_h and ϕ_p, we should expect the state with the lowest energy is chosen. Therefore, the gauge current would show the same periodicity in both phases, while in the ordered phase it will show discontinuities accompanied with parity switches reflected in the sign reversals of the maximal multipoint spin-z correlator.

Numerical results.—To demonstrate these effects concretely, we have calculated the gauge current by exact diagonalization of the Floquet Hamiltonian in (7) and (8). In Fig. 3, we plot the average current $j_b^{(0)} = j_L^{(0)} + j_R^{(0)}$ through the bridge for a representative set of parameters realizing the trivial and topological phases of fermions as a function of gauge parameters ϕ_h and ϕ_p. Here, we have chosen $|\Phi_0\rangle$ as the lowest energy state of the whole system. In the trivial phase, the current scales with w_b^2 and since both $w_b, \Delta_b \neq 0$, compared to the conventional Josephson junction with $\Delta_b = 0$, the periodicity in ϕ_p and ϕ_h is doubled. In the topological phase, the current scales with w_b and its discontinuities coincide with parity switches, as expected. Note that except for discontinuous jumps due to parity switches in P_0, $j_b = 2P_0F_{cs}\sin\phi_p$ has no other dependence on ϕ_h.

The magnetization current of the Floquet gauge pump realized in the driven XY model is shown in Fig. 4 as a

function of phase shifts $\theta_a^h - \theta^J$ across the bridge. Note that, as these drive parameters are varied, both phases ϕ_h and ϕ_p as well as the amplitudes w_b, Δ_b, w_a, and Δ_a change in a range determined by the drive amplitudes. We discuss this dependence in the Supplemental Material [33]. The difference between disordered [Fig. 4(a)] and ordered [Fig. 4(b)] phases is that there is a true discontinuous change in the current in Fig. 4(b), while the change in Fig. 4(a) is gradual. The sign of the maximal multipoint spin-z correlator provides a complementary signature of ground-state degeneracy.

Experimental realization.—The Floquet gauge pump can be realized using trapped atomic ions, which are a well-established system for simulating the time evolution of spin-lattice Hamiltonians [66]. Ions form defect-free lattices and can support quantum coherence times of longer than 10 min [67]. Interactions between ions—which map to interactions between effective quantum spins—can be fully controlled and reprogrammed using laser light [68]. These features have made trapped ions the leading platform for establishing atomic frequency standards [69] and for performing quantum simulations of 1D spin chains.

All necessary components for implementing the Floquet gauge pump have been previously demonstrated in trapped-ion systems. Transverse-field Ising and XY models are routinely generated by driving stimulated Raman transitions between the effective spin states [70,71]. The resulting spin model depends upon the specific amplitude, frequency, and phase characteristics of the Raman laser beams, which can be controlled by passing the beams through an acousto-optic modulator (AOM) [72]. Periodically driving the amplitude of the rf signal applied to the AOMs will imprint itself as a periodic drive on the spin-spin couplings $\{J^x(t), J^y(t)\}$ and transverse fields $h^z(t)$; indeed, this technique has already been used to realize Floquet engineering of a trapped-ion crystal [73]. The one key challenge will be to implement asymmetric drives on the left and right halves of the chain. This may be solved by either (i) adding a second pair of Raman beams so that both halves can be independently addressed, or by (ii) adding a second pair of frequency components to the AOM rf drive to split a single Raman beam into two parts, each with its own amplitude, frequency, phase, and deflection angle.

Topological degeneracies are detected by discontinuities in $d\langle S^z(t)\rangle/dt$. At high frequencies $\Omega \sim$ MHz in Fig. 4, $d\langle S^z(t)\rangle/dt \sim 100$ Hz (see [33]). Full contrast is obtained over $\sim$10 ms. High resolution of 1 part in 1000 in θ^h is also easily achieved. A strength of trapped-ion systems is the ability to perform site-resolved spin-dependent fluorescence, which acts as a projective measurement along the z direction and can discriminate between spin states with $> 99.9\%$ fidelity [74]. Since all effective spins are detected simultaneously during the measurement, all possible spin correlators (including the N-body correlator $\langle S_1^z S_2^z, \ldots, S_N^z\rangle$) can be reconstructed when repeated trials are averaged.

Concluding remarks.—Dynamical probes to interrogate and uncover the emergent discrete symmetries that give rise to ground-state degeneracies are key to discovering topological or broken-symmetry phases of matter. The Floquet gauge pump we have introduced in this Letter is a unique experimental tool conceiving this goal.

Although our proposed proof-of-principle implementation in an ion-trap platform involved simple many-body systems, we expect that the Floquet gauge pump becomes a routine technique even in complex interacting systems. The required ingredient is the existence of the gauge group. A sufficient condition in the spin models is the absence of couplings between the directions parallel and perpendicular to the field. The gauge group is then the rotations around the field, which relabels the axes in the perpendicular direction and leaves the spectrum unchanged. In the XY model, for example, we can see immediately that the gauge pump works just as well in the presence of S^z-dependent interactions for spins [75,76], since these operators commute with the gauge current [33]. In practical setups of ion-trap simulators, tunable, variable-range interactions between effective spin degrees of freedom are realized, also in two-dimensional geometries [77], adding the possibility of magnetic frustration and potentially leading to exotic quantum spin liquid phases. Moreover, unveiling discrete symmetries can help in understanding the mechanisms leading to the formation of localized many-body boundary modes [11,13,24]. This is of fundamental importance for practical applications, in particular, if the vacuum is topological and those modes represent quasiparticles with non-Abelian braiding statistics.

This work is supported primarily by the U.S. Department of Energy, Office of Science, Basic Energy Sciences, under Award No. DE-SC0020343. B. S. and A. K. were supported in part by NSF CAREER Grant No. DMR-1350663 (early work on Floquet Hamiltonians).

[1] A. P. Schnyder, S. Ryu, A. Furusaki, and A. W. W. Ludwig, Classification of topological insulators and superconductors in three spatial dimensions, Phys. Rev. B **78**, 195125 (2008).
[2] A. Kitaev, V. Lebedev, and M. Feigel'man, Periodic table for topological insulators and superconductors, in *AIP Conference Proceedings, Proceedings of the L. D. Landau Memorial Conference "Advances in Theoretical Physics," 2008* (AIP, New York, 2009).
[3] J. C. Y. Teo and C. L. Kane, Topological defects and gapless modes in insulators and superconductors, Phys. Rev. B **82**, 115120 (2010).
[4] S. Ryu, A. P. Schnyder, A. Furusaki, and A. W. W. Ludwig, Topological insulators and superconductors: Tenfold way and dimensional hierarchy, New J. Phys. **12**, 065010 (2010).
[5] L. Fu, Topological Crystalline Insulators, Phys. Rev. Lett. **106**, 106802 (2011).

[6] L. Isaev, Y. H. Moon, and G. Ortiz, Bulk-boundary correspondence in three-dimensional topological insulators, Phys. Rev. B **84**, 075444 (2011).

[7] E. Prodan and H. Schulz-Baldes, *Bulk and Boundary Invariants for Complex Topological Insulators* (Springer International Publishing, New York, 2016).

[8] K. T. Law, P. A. Lee, and T. K. Ng, Majorana Fermion Induced Resonant Andreev Reflection, Phys. Rev. Lett. **103**, 237001 (2009).

[9] J. Liu, A. C. Potter, K. T. Law, and P. A. Lee, Zero-Bias Peaks in the Tunneling Conductance of Spin-Orbit-Coupled Superconducting Wires with and without Majorana End-States, Phys. Rev. Lett. **109**, 267002 (2012).

[10] G. Goldstein and C. Chamon, Exact zero modes in closed systems of interacting fermions, Phys. Rev. B **86**, 115122 (2012).

[11] G. Ortiz, J. Dukelsky, E. Cobanera, C. Esebbag, and C. Beenakker, Many-Body Characterization of Particle-Conserving Topological Superfluids, Phys. Rev. Lett. **113**, 267002 (2014).

[12] G. Kells, Many-body Majorana operators and the equivalence of parity sectors, Phys. Rev. B **92**, 081401(R) (2015).

[13] G. Ortiz and E. Cobanera, What is a particle-conserving topological superfluid? The fate of Majorana modes beyond mean-field theory, Ann. Phys. (Amsterdam) **372**, 357 (2016).

[14] E. Grosfeld, B. Seradjeh, and S. Vishveshwara, Proposed Aharonov-Casher interference measurement of non-Abelian vortices in chiral p-wave superconductors, Phys. Rev. B **83**, 104513 (2011).

[15] F. Hassler, A. R. Akhmerov, C.-Y. Hou, and C. W. J. Beenakker, Anyonic interferometry without anyons: How a flux qubit can read out a topological qubit, New J. Phys. **12**, 125002 (2010).

[16] E. Grosfeld and A. Stern, Observing Majorana bound states of Josephson vortices in topological superconductors, Proc. Natl. Acad. Sci. U.S.A. **108**, 11810 (2011).

[17] S. Bose and P. Sodano, Nonlocal Hanbury-Brown-Twiss interferometry and entanglement generation from Majorana bound states, New J. Phys. **13**, 085002 (2011).

[18] J. Alicea, New directions in the pursuit of Majorana fermions in solid state systems, Rep. Prog. Phys. **75**, 076501 (2012).

[19] D. Dahan, M. T. Ahari, G. Ortiz, B. Seradjeh, and E. Grosfeld, Non-Abelian fermion parity interferometry of Majorana bound states in a Fermi sea, Phys. Rev. B **95**, 201114(R) (2017).

[20] A. Y. Kitaev, Unpaired Majorana fermions in quantum wires, Phys. Usp. **44**, 131 (2001).

[21] H.-J. Kwon, K. Sengupta, and V. H. Yakovenko, Theoretical prediction of the fractional ac Josephson effect in p- and d-wave superconductors, Braz. J. Phys. **33**, 653 (2003).

[22] L. Fu and C. L. Kane, Josephson current and noise at a superconductor/quantum-spin-Hall-insulator/superconductor junction, Phys. Rev. B **79**, 161408(R) (2009).

[23] L. P. Rokhinson, X. Liu, and J. K. Furdyna, The fractional a.c. Josephson effect in a semiconductor-superconductor nanowire as a signature of Majorana particles, Nat. Phys. **8**, 795 (2012).

[24] E. Cobanera and G. Ortiz, Fock parafermions and self-dual representations of the braid group, Phys. Rev. A **89**, 012328 (2014).

[25] E. Cobanera, J. Ulrich, and F. Hassler, Changing anyonic ground degeneracy with engineered gauge fields, Phys. Rev. B **94**, 125434 (2016).

[26] P. Jordan and E. Wigner, On the Pauli exclusion principle, Z. Phys. **47**, 631 (1928).

[27] For other examples of spatial variation in a Floquet drive, see Refs. [28–30].

[28] Y. T. Katan and D. Podolsky, Modulated Floquet Topological Insulators, Phys. Rev. Lett. **110**, 016802 (2013).

[29] A. Kundu, H. A. Fertig, and B. Seradjeh, Floquet-Engineered Valleytronics in Dirac Systems, Phys. Rev. Lett. **116**, 016802 (2016).

[30] M. Rodriguez-Vega, A. Kumar, and B. Seradjeh, Higher-order Floquet topological phases with corner and bulk bound states, Phys. Rev. B **100**, 085138 (2019).

[31] By contrast, a topological quantum pump such as the Thouless pump [32] is realized by an adiabatic cycle of the Hamiltonian that breaks the symmetry underlying the topological phase and pumps a quantized number of topological boundary modes through the system, resulting in a current flow.

[32] D. J. Thouless, Quantization of particle transport, Phys. Rev. B **27**, 6083 (1983).

[33] See Supplemental Material at http://link.aps.org/supplemental/10.1103/PhysRevLett.126.206602 for details of gauge current, Floquet gauge current, Floquet Hamiltonian of driven XY model, time-averaged Floquet gauge current in the driven XY and equivalent fermion model, and additional numerical results.

[34] T. Oka and H. Aoki, Photovoltaic Hall effect in graphene, Phys. Rev. B **79**, 081406(R) (2009).

[35] Y. H. Wang, H. Steinberg, P. Jarillo-Herrero, and N. Gedik, Observation of Floquet-Bloch states on the surface of a topological insulator, Science **342**, 453 (2013).

[36] Á. Gómez-León, P. Delplace, and G. Platero, Engineering anomalous quantum Hall plateaus and antichiral states with ac fields, Phys. Rev. B **89**, 205408 (2014).

[37] A. Poudel, G. Ortiz, and L. Viola, Dynamical generation of Floquet Majorana flat bands in s-wave superconductors, Europhys. Lett. **110**, 17004 (2015).

[38] J. W. McIver, B. Schulte, F.-U. Stein, T. Matsuyama, G. Jotzu, G. Meier, and A. Cavalleri, Light-induced anomalous Hall effect in graphene, Nat. Phys. **16**, 38 (2020).

[39] G. E. Topp, G. Jotzu, J. W. McIver, L. Xian, A. Rubio, and M. A. Sentef, Topological Floquet engineering of twisted bilayer graphene, Phys. Rev. Research **1**, 023031 (2019).

[40] Y. Li, H. A. Fertig, and B. Seradjeh, Floquet-engineered topological flat bands in irradiated twisted bilayer graphene, Phys. Rev. Research **2**, 043275 (2020).

[41] O. Katz, G. Refael, and N. H. Lindner, Optically induced flat bands in twisted bilayer graphene, Phys. Rev. B **102**, 155123 (2020).

[42] M. Rodriguez-Vega, M. Vogl, and G. A. Fiete, Low-frequency and Moiré Floquet engineering: A review, Ann. Phys., https://doi.org/10.1016/j.aop.2021.168434.

[43] T. Ozawa, H. M. Price, A. Amo, N. Goldman, M. Hafezi, L. Lu, M. C. Rechtsman, D. Schuster, J. Simon, O. Zilberberg *et al.*, Topological photonics, Rev. Mod. Phys. **91**, 015006 (2019).
[44] T. Oka and S. Kitamura, Floquet engineering of quantum materials, Annu. Rev. Condens. Matter Phys. **10**, 387 (2019).
[45] M. S. Rudner and N. H. Lindner, The Floquet engineer's handbook, arXiv:2003.08252.
[46] M. S. Rudner and N. H. Lindner, Band structure engineering and non-equilibrium dynamics in Floquet topological insulators, Nat. Rev. Phys. **2**, 229 (2020).
[47] G. Floquet, Sur les équations différentielles linéaires à coefficients périodiques, Ann. Sci. Ecolé Norm. Sup. **12**, 47 (1883).
[48] J. H. Shirley, Solution of the Schrödinger equation with a Hamiltonian periodic in time, Phys. Rev. **138**, B979 (1965).
[49] H. Sambe, Steady states and quasienergies of a quantum-mechanical system in an oscillating field, Phys. Rev. A **7**, 2203 (1973).
[50] A. Eckardt and E. Anisimovas, High-frequency approximation for periodically driven quantum systems from a Floquet-space perspective, New J. Phys. **17**, 093039 (2015).
[51] M. Rodriguez-Vega, M. Lentz, and B. Seradjeh, Floquet perturbation theory: Formalism and application to low-frequency limit, New J. Phys. **20**, 093022 (2018).
[52] L. D'Alessio and M. Rigol, Long-Time Behavior of Isolated Periodically Driven Interacting Lattice Systems, Phys. Rev. X **4**, 041048 (2014).
[53] A. Lazarides, A. Das, and R. Moessner, Equilibrium states of generic quantum systems subject to periodic driving, Phys. Rev. E **90**, 012110 (2014).
[54] A. Lazarides, A. Das, and R. Moessner, Periodic Thermodynamics of Isolated Quantum Systems, Phys. Rev. Lett. **112**, 150401 (2014).
[55] A. Lazarides, A. Das, and R. Moessner, Fate of Many-Body Localization under Periodic Driving, Phys. Rev. Lett. **115**, 030402 (2015).
[56] P. Ponte, A. Chandran, Z. Papić, and D. A. Abanin, Periodically driven ergodic and many-body localized quantum systems, Ann. Phys. (Amsterdam) **353**, 196 (2015).
[57] P. Ponte, Z. Papić, F. Huveneers, and D. A. Abanin, Many-Body Localization in Periodically Driven Systems, Phys. Rev. Lett. **114**, 140401 (2015).
[58] V. Khemani, A. Lazarides, R. Moessner, and S. L. Sondhi, On the Phase Structure of Driven Quantum Systems, Phys. Rev. Lett. **116**, 250401 (2016).
[59] T. Mori, T. Kuwahara, and K. Saito, Rigorous Bound on Energy Absorption and Generic Relaxation in Periodically Driven Quantum Systems, Phys. Rev. Lett. **116**, 120401 (2016).
[60] T. Kuwahara, T. Mori, and K. Saito, Floquet-Magnus theory and generic transient dynamics in periodically driven many-body quantum systems, Ann. Phys. (Amsterdam) **367**, 96 (2016).
[61] D. Abanin, W. De Roeck, W. W. Ho, and F. Huveneers, A rigorous theory of many-body prethermalization for periodically driven and closed quantum systems, Commun. Math. Phys. **354**, 809 (2017).
[62] S. A. Weidinger and M. Knap, Floquet prethermalization and regimes of heating in a periodically driven, interacting quantum system, Sci. Rep. **7**, 45382 (2017).
[63] N. H. Lindner, E. Berg, and M. S. Rudner, Universal Chiral Quasisteady States in Periodically Driven Many-Body Systems, Phys. Rev. X **7**, 011018 (2017).
[64] C.-K. Chiu and S. Das Sarma, Fractional Josephson effect with and without Majorana zero modes, Phys. Rev. B **99**, 035312 (2019).
[65] L. Jiang, D. Pekker, J. Alicea, G. Refael, Y. Oreg, and F. von Oppen, Unconventional Josephson Signatures of Majorana Bound States, Phys. Rev. Lett. **107**, 236401 (2011).
[66] C. Monroe, W. Campbell, L.-M. Duan, Z.-X. Gong, A. Gorshkov, P. Hess, R. Islam, K. Kim, G. Pagano, P. Richerme, C. Senko, and N. Yao, Programmable quantum simulations of spin systems with trapped ions, Rev. Mod. Phys. **93**, 025001 (2021).
[67] Y. Wang, M. Um, J. Zhang, S. An, M. Lyu, J.-N. Zhang, L.-M. Duan, D. Yum, and K. Kim, Single-qubit quantum memory exceeding ten-minute coherence time, Nat. Photonics **11**, 646 (2017).
[68] K. Mølmer and A. Sørensen, Multiparticle Entanglement of Hot Trapped Ions, Phys. Rev. Lett. **82**, 1835 (1999).
[69] A. D. Ludlow, M. M. Boyd, J. Ye, E. Peik, and P. O. Schmidt, Optical atomic clocks, Rev. Mod. Phys. **87**, 637 (2015).
[70] P. Richerme, Z.-X. Gong, A. Lee, C. Senko, J. Smith, M. Foss-Feig, S. Michalakis, A. V. Gorshkov, and C. Monroe, Non-local propagation of correlations in quantum systems with long-range interactions, Nature (London) **511**, 198 (2014).
[71] P. Jurcevic, B. P. Lanyon, P. Hauke, C. Hempel, P. Zoller, R. Blatt, and C. F. Roos, Quasiparticle engineering and entanglement propagation in a quantum many-body system, Nature (London) **511**, 202 (2014).
[72] A. C. Lee, J. Smith, P. Richerme, B. Neyenhuis, P. W. Hess, J. Zhang, and C. Monroe, Engineering large Stark shifts for control of individual clock state qubits, Phys. Rev. A **94**, 042308 (2016).
[73] J. Zhang, P. Hess, A. Kyprianidis, P. Becker, A. Lee, J. Smith, G. Pagano, I.-D. Potirniche, A. C. Potter, A. Vishwanath *et al.*, Observation of a discrete time crystal, Nature (London) **543**, 217 (2017).
[74] R. Noek, G. Vrijsen, D. Gaultney, E. Mount, T. Kim, P. Maunz, and J. Kim, High speed, high fidelity detection of an atomic hyperfine qubit, Opt. Lett. **38**, 4735 (2013).
[75] L. Herviou, C. Mora, and K. Le Hur, Phase diagram and entanglement of two interacting topological Kitaev chains, Phys. Rev. B **93**, 165142 (2016).
[76] I. Mahyaeh and E. Ardonne, Study of the phase diagram of the Kitaev-Hubbard chain, Phys. Rev. B **101**, 085125 (2020).
[77] M. D'Onofrio, Y. Xie, A. J. Rasmusson, E. Wolanski, J. Cui, and P. Richerme, Radial two-dimensional ion crystals in a linear Paul trap, arXiv:2012.12766.